CHIN. PHYS. LETT. Vol. 35, No. 7 (2018) 076801

An Efficiency Enhanced Graphene/n-Si Schottky Junction for Solar Cells *

Gang Li(李刚)[1], Hong-Wei Cheng(程宏伟)[1], Li-Fang Guo(郭丽芳)[1],
Kai-Ying Wang(王开鹰)[1**], Zai-Jun Cheng(程再军)[2**]

[1]*MicroNano System Research Center, College of Information and Computer & Key Lab of Advanced Transducers and Intelligent Control System of Ministry of Education, Taiyuan University of Technology, Taiyuan 030024*
[2]*School of Optoelectronic and Communication Engineering, Xiamen University of Technology, Xiamen 361024*

(Received 8 March 2018)

A novel and facile oxidation-induced self-doping process of graphene-silicon Schottky junction by nitric acid (HNO_3) vapor is reported. The HNO_3 oxidation process makes graphene p-type self-doped, and leads to a higher built-in potential and conductivity to enhance charge transfer and to suppress charge carrier recombination at the graphene-silicon Schottky junction. After the HNO_3 oxidation process, the open-circuit voltage is increased from the initial value of 0.36 V to the maximum value of 0.47 V, the short-circuit current is greatly increased from 0.80 μA to 7.71 μA, and the ideality factor is optimized from 4.4 to 1.0. The enhancement of the performance of graphene-Si solar cells may be due to oxidation-induced p-type self-doping of graphene-Si junctions.

PACS: 68.65.Pq, 88.40.jj, 88.40.H– DOI: 10.1088/0256-307X/35/7/076801

Solar energy, with the merits of no pollution, abundance on the Earth and mature technology, is one of the most promising renewable energy sources. Schottky barrier solar cells, normally formed by contacting a metal with a moderate doped semiconductor, are extensively studied due to their merits of material universality, low cost, and easy fabrication.[1] At present, silicon based devices dominate the commercial photovoltaic market due to its abundant material resources, well-established manufacturing techniques, high carrier mobility, and low leakage current. In a conventional Schottky junction solar cell, the thick conductive metal layer limits the efficiency of energy conversion, because the metal layer should be thick enough to form a continuous film, which always absorbs and reflects most of the solar radiation.[2] ITO is a conventional material and is widely used for front electrode in solar cells,[3] while the limited resource of indium leads to the rising cost of production, and their transmittance at the ultraviolet region, chemical and electronic stability, and mechanical flexibility limit their application in flexible optoelectronic devices.[4] Therefore, new materials such as carbon nanotubes,[5] titanium dioxides,[6] conducting polymers,[7] and molybdenum disulfide,[8] are continually applied to solar cells for the purpose of exploiting new photo-electrical conversion systems or enhancing the solar cell performance. Among them, graphene is one of the most attractive and promising materials to replace ITO because of its two-dimensional characteristics, high mobility,[9] near-zero band-gap,[10] high transmittance within the ultraviolet–visible region,[11] high electrical conductivity,[12] and outstanding flexibility and stability.[13,14] Specially, the success in growing a large-scale high-quality few layer graphene by the chemical vapor deposition method (CVD) using a Ni or Cu catalyst enables researchers to readily apply it to optoelectronic devices.[15] The synthesized CVD graphene film can be transferred to an arbitrary target substrate using polymethyl methacrylate (PMMA) or polydimethylsiloxine (PDMS). Thus graphene can replace ITO to obtain better electrical and optical performance[16] and is promising in serving as a transparent conductive film. Therefore, graphene-Si Schottky junctions are desired to construct a solar cell, in which graphene films not only play the role of a transparent electrode for light transmission, charge collection, and transport, but also acts as an active component to participate in the photogeneration process.[17] However, the photoelectrical energy conversion of a graphene-silicon solar cell is still low because of the poor electrical properties of graphene.[18] The approaches such as adjusting the layer number of graphene[19], and using a silicon-pillar-array[20] and antireflection treatments[21] have been developed to improve the performance of graphene-Si solar cells, while these approaches always suffer from high cost and a complicated fabrication process. Thus developing an effective and facile approach is still desired to enhance the photovoltaic performance of graphene-silicon Schottky junction solar cells.

In this work, a few-layer CVD graphene film is transferred onto an n-type silicon substrate to form a graphene-silicon Schottky junction solar cell. A facile surface p-type self-doping of graphene film is employed to enhance the conductivity of the graphene film and the built-in potential of the graphene-silicon Schot-

*Supported by the National Natural Science Foundation of China under Grant Nos 61504113, 61674113 and 51622507, the Natural Science Foundation of Shanxi Province under Grant No 2016011040, the Natural Science Foundation of Fujian Province under Grant No 2018J01567, and the Scientific and Technological Innovation Programs of Higher Education Institutions in Shanxi Province under Grant No 2016138.

**Corresponding author. Email: Kaiying.Wang@usn.no; 2011111002@xmut.edu.cn

© 2018 Chinese Physical Society and IOP Publishing Ltd

tky junction by means of the HNO_3 vapor oxidation process. The HNO_3 vapor processed graphene film is characterized by scanning electron microscopy (SEM) and Raman spectroscopy. The photovoltaic properties such as open-circuit voltage and short-circuit current are studied before and after oxidation self-doping of the graphene film. The performance-enhanced mechanisms of the graphene-silicon Schottky junction will be discussed for solar cells before and after oxidation-induced self-doping of the graphene film.

Figure 1 shows the process flow of graphene-silicon Schottky junction solar cells. A single crystal n-Si (100) wafer (1–5 Ω·cm) with 285 nm silicon oxide (SiO_2) was used as the starting substrate. Then, SiO_2 was partly opened using a buffered oxide etch (BOE) with NH_4F/HF (6:1) ratio for 5 min to expose the underlying Si. The as-prepared Si substrate was respectively cleaned in acetone, ethanol, and deionized water in an ultrasound bath for 15 min. Then, the synthesized CVD graphene film grown on copper foil was transferred onto the silicon substrate. The graphene/Cu foil was firstly transferred onto a physical support of poly-methyl methacrylate (PMMA). Then, the copper foil was etched from the formed PMMA/graphene/Cu foil using an aqueous ammonium persulfate ($(NH_4)_2S_2O_8$) etchant solution, yielding PMMA/graphene foil. After that, the PMMA/graphene foil floating on the solution was transferred to the target silicon substrate. Subsequently, the graphene film was rinsed with deionized water after the PMMA supporting layer was dissolved away in an acetone solution.

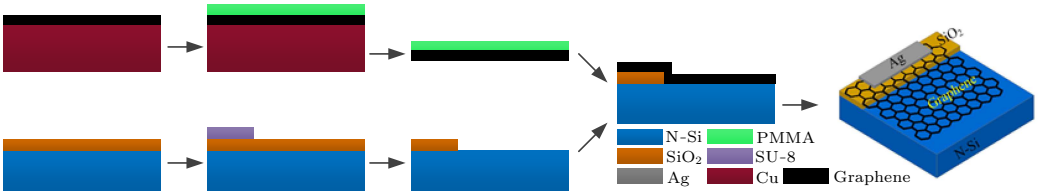

Fig. 1. Process flow of graphene-silicon Schottky junction solar cells.

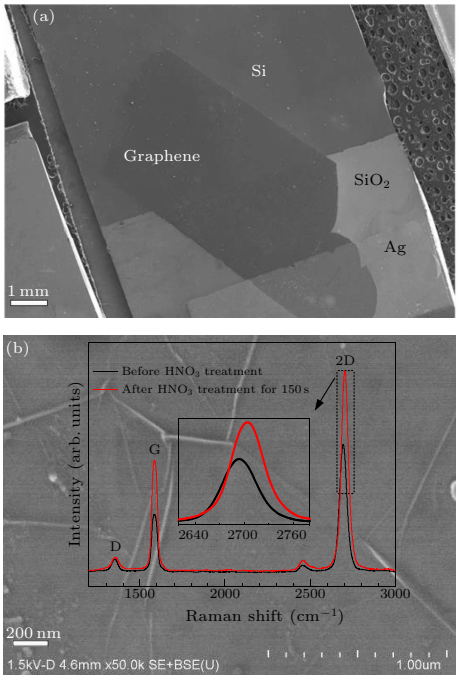

Fig. 2. (a) A top-view SEM image of a graphene film transferred onto the Si substrate. (b) A top-view SEM image of a graphene film transferred onto the Si substrate (the inset is the Raman spectra of the graphene film).

An annealing process was performed to remove further residues at 400℃ with Ar (∼500 sccm) and H_2 (∼500 sccm) for 40 min. Finally, conducting silver paste coating was performed to form the top and bottom electrodes for the graphene-Si solar cell. Furthermore, the HNO_3 vapor oxidation process was carried out by placing the solar cell above a vial containing HNO_3 at ambient temperature for different treatment times. The as-prepared graphene-Si solar cell was characterized by SEM and Raman spectroscopy. The current-voltage (I–V) curves were measured using a Keithley 2400 source meter. All photovoltaic performance tests were performed with an Xe lamp (PLS-SXE300) in air ambient at room temperature.

Figure 2(a) shows the SEM image of the graphene-Si solar cell. Clearly, the graphene film was continuous between the SiO_2 layer and Si channel to form the Schottky junction. The graphene film could adhere tightly to the Si substrate without air bubbles at the interface of the junction. Furthermore, some wrinkles of the graphene film formed during the graphene transfer processes could be observed as shown in Fig. 2(b). Moreover, the Raman spectroscopy of the graphene film before and after HNO_3 processing can be analyzed shown in the inset of Fig. 2(b). Most of the intense features of G and 2D peaks could be observed in the Raman spectrum. The D peak is caused by the breathing modes of six-atom rings and requires a defect for its activation,[22] whereas the G band arises from the doubly degenerate E_{2g} mode at the Brillouin zone center. The intensity ratio of the G to 2D bands is about 0.59, indicating that the graphene film is composed of an average of 2–4 layers.[23] Interestingly, the HNO_3 treated graphene film exhibits a continuous blue shift of G and 2D peaks. The G peak shifts from the initial 1584.0 cm^{-1} to 1585.6 cm^{-1}, which indicates electron transfer from pristine graphene to the dopant.[24] However, there is no splitting of the G peak after the HNO_3 processing, indicating that the dopant is mainly from

chemical adsorbing and interacting with the surface rather than intercalating.[25] The 2D peak shifts from 2692.8 cm^{-1} to 2704.0 cm^{-1}, which indicates that the HNO_3 oxidation process makes the graphene films p-type doped.[26]

The p-type self-doping process of graphene film could be explained according to the following equation

$$6HNO_3 + 25C \rightarrow C_{25}^{+}NO_3 \cdot 4HNO_3 + NO_2 + H_2O. \quad (1)$$

The reaction mechanism shows that electrons are transferred from the graphene film to HNO_3 and therefore the graphene film will be slightly oxidized, which will lead to a p-type self-doping of the graphene film. Correspondingly, the Fermi energy level and electrical conductivity of the graphene film will be modified by p-type self-doping.

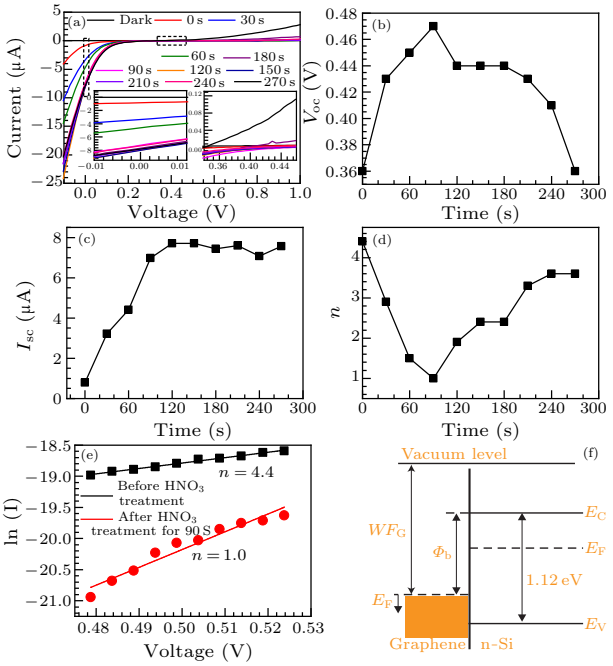

Fig. 3. (a) The I–V characteristics of the graphene-Si solar cell under dark and light for different HNO_3 processing times from 0 to 270 s, processing time versus (b) open-circuit voltage, (c) short-circuit current, (d) ideality factor, (e) ideality factor with and without HNO_3 processing for 150 s, and (f) energy band diagram at the graphene-Si interface.

Figure 3(a) shows the I–V characteristics of the graphene-Si solar cell under dark and light for different HNO_3 processing times from 0 to 270 s. Clearly, the photovoltaic properties are significantly dependent on the HNO_3 oxidation processes. To further evaluate the effect of HNO_3 oxidation processes, the photovoltaic parameters of the graphene-Si solar cell can be extracted in terms of open-circuit voltage (V_{oc}), short-circuit current (I_{sc}), and ideality factor (n) from the I–V curves. Figure 3(b) shows the effects of the HNO_3 processing time on the open-circuit voltage of the graphene-Si solar cell. It is found that V_{oc} increases sharply at the beginning of the HNO_3 oxidization process and reaches a maximum value of 0.47 V at the processing time of 90 s. Then, V_{oc} decreases to 0.44 V and remains for a period. Finally, it decreases to the original value of 0.36 V. Figure 3(c) shows that the short circuit current changes as a function of the HNO_3 processing time. It is seen that I_{sc} (0.80 μA) increases dramatically at the beginning of processing and then saturates close to the maximum value of 7.71 μA.

The ideality factor n, which could be extracted from the slope of dark log-scale I–V plots of the graphene-Si Schottky junction follows

$$n = q/kTdV/d\ln J, \quad (2)$$

where q is the electron charge, T is the temperature, k is the Boltzmann constant, V is the forward voltage, and J is the current density.[27] The ideality factor is firstly calculated and plotted as a function of the HNO_3 treating time. As shown in Fig. 3(d), it is noted that the ideality factor n decreases firstly to a minimum value at the processing time of 90 s, and then increases with the HNO_3 processing time. The result indicates that the quality of Schottkey junction gets better, and then gets worse during the HNO_3 oxidization process. Clearly, the ideality factor is calculated to be 4.4 before HNO_3 processing while 1.0 after the processing time of 90 s as shown in Fig. 3(e), further suggesting that the charge carrier recombination at the Schottky junction interface can be suppressed by proper HNO_3 processing.[28]

The enhanced photovoltaic performance could be attributed to the optimized Fermi energy level and electrical conductivity of graphene by the HNO_3 processing. As mentioned above, the HNO_3 processing could make graphene p-type doped, which will lead to a lower Fermi energy level and higher conductivity of graphene. As shown in Fig. 3(f), the Fermi energy level of graphene will strongly influence the built-in potential V_{bi} at the graphene-Si Schottky junction, which can be expressed as[29]

$$V_{bi} = \Phi_b - \exp(-1)kT\ln(N_C/N_D), \quad (3)$$

where Φ_b is the Schottky-barrier height, N_C is the effective density of states in the conduction band, and N_D is the self-doping level of the semiconductor. After HNO_3 processing, a lower Fermi energy level of graphene will lead to a higher Φ_b, resulting in a higher built-in potential V_{bi}, which will enhance charge transfer and will suppress charge carrier recombination. Thus V_{oc} increases while n decreases at the beginning of the HNO_3 oxidization process. However, the excess HNO_3 processing may introduce new defects functioning as a recombination center, which leads to the decrease of V_{oc} and the increase of n at the latter stage of the HNO_3 oxidization process. Furthermore, the surface p-type self-doping will significantly increase the graphene conductivity until the self-doping reaches saturation by HNO_3 processing. Thus I_{sc} increases

firstly and then almost reaches stability during the HNO_3 oxidization process.

In conclusion, the photovoltaic performance of a graphene-silicon Schottky junction has been investigated before and after chemical-oxidation self-doping of the graphene film for solar cells. The experimental results show that the open-circuit voltage (V_{oc}), short-circuit current (I_{sc}), and ideality factor (n) are significantly dependent on the self-doping processes of graphene. The enhanced photovoltaic properties of graphene-silicon Schottky junction solar cells are attributed to the lower Fermi energy level and higher electrical conductivity of graphene by surface p-type self-doping of the graphene film by means of HNO_3 processing.

References

[1] Wang Y S, Chen C Y, Fang X, Li Z P, Qiao H, Sun B Q and Bao Q L 2015 *J. Solid State Chem.* **224** 102
[2] Ye Y and Da L 2012 *J. Mater. Chem.* **22** 24224
[3] Tang J, Wang X H, Brzozowski L, Barkhouse D A R, Debnath R, Levina L and Sargent E 2010 *Adv. Mater.* **22** 1398
[4] Sun Y Q, Wu Q and Shi G Q 2011 *Energy Environ. Sci.* **4** 1113
[5] Jensen S A, Ulbricht R, Narita A, Feng X L, Müllen K, Hertel T, Turchinovich D and Bonn M 2013 *Nano Lett.* **13** 5925
[6] Liu G H, Hoivik N, Wang X M, Lu S S, Wang K Y and Jakobsen H 2013 *Electrochim. Acta* **93** 80
[7] Sun H P et al 2014 *Electrochim. Acta* **137** 661
[8] Zhao P X, Tang Y, Mao J, Chen Y X, Song H, Wang J W, Song Y, Liang Y Q and Zhang X M 2016 *J. Alloys Compd.* **674** 252
[9] Novoselov K S, Geim A K, Morozov S V, Jiang D, Zhang Y, Dubonos S V, Grigorieva I V and Firsov A A 2004 *Science* **306** 666
[10] Xing G C, Guo H C, Zhang X H, Sum T C and Huan C H A 2010 *Opt. Express* **18** 4564
[11] Wang T S, Liu Z H, Lu M M, Wen B, Ouyang Q Y, Chen Y J, Zhu C L, Gao P, Li C Y, Cao M S and Qi L H 2013 *J. Appl. Phys.* **113** 666
[12] Li X S, Zhu Y W, Cai W W, Borysiak M, Han B, Chen D, Piner R D, Colombo L and Ruoff R S 2009 *Nano Lett.* **9** 4359
[13] Fan X B, Peng W C, Li Y, Li X Y, Wang S L, Zhang G L and Zhang F B 2008 *Adv. Mater.* **20** 4490
[14] Lee G H, Yu Y J, Cui X, Petrone N, Lee C H, Choi M S, Lee D Y, Lee C, Yoo W J, Watanabe K, Taniguchi T, Nuckolls C, Kim P and Hone J 2013 *ACS Nano* **7** 7931
[15] Kim K S, Zhao Y, Jang H, Lee S Y, Kim J M, Kim K S, Ahn J H, Kim P, Choi J Y and Hong B H 2009 *Nature* **457** 706
[16] Li C, Moncorgé R, Wyon C and Aubert J 2013 *Advanced Solid State Lasers* (Boston: OSA)
[17] Li X M, Zhu H W, Wang K L, Cao A Y, Wei J Q, Li C Y, Jia Y, Li Z, Li X and Wu D H 2010 *Adv. Mater.* **22** 2743
[18] Yin C R, Ye S H, Zhao J, Yi M D, Xie L H, Lin Z Q, Chang Y Z, Liu F, Xu H, Shi N E, Qian Y and Huang W 2011 *Macromolecules* **44** 4589
[19] Li Y F, Yang W, Tu Z Q, Liu Z C, Yang F, Zhang L Q and Hatakeyama R 2014 *Appl. Phys. Lett.* **104** 043903
[20] Feng T T, Xie D, Lin Y X, Zang Y Y, Ren T L, Song R, Zhao H M, Tian H, Li X, Zhu H M and Liu L T 2011 *Appl. Phys. Lett.* **99** 233505
[21] Lancellotti L, Bobeico E, Capasso A, Lago E, Veneri P D, Leoni E, Buonocore F and Lisi N 2016 *Sol. Energy* **127** 198
[22] Basko D M, Piscanec S and Ferrari A C 2009 *Phys. Rev.* B **80** 165413
[23] Das A, Chakraborty B, Piscanec S, Pisana S, Sood A K and Ferrari A C 2009 *Phys. Rev.* B **79** 155417
[24] Wassei J K, Cha K C, Tung V C, Yang Y and Kaner R B 2011 *J. Mater. Chem.* **21** 3391
[25] Allen M J, Wang M, Jannuzzi S A, Yang Y, Wang K L and Kaner R B 2009 *Chem. Commun.* **41** 6285
[26] Ni Z H, Wang Y Y, Yu T and Shen Z X 2008 *Nano Res.* **1** 273
[27] Dahal R, Pantha B, Li J, Lin J Y and Jiang H X 2009 *Appl. Phys. Lett.* **94** 063505
[28] Shi E Z, Li H B, Yang L, Zhang L H, Li Z, Li P X, Shang Y Y, Wu S T, Li X M, Wei J Q, Wang K L, Zhu H M, Wu D H, Fang Y and Cao A Y 2013 *Nano Lett.* **13** 1776
[29] Sze S M 2008 *Physics of Semiconductor Devices* 3nd edn (Xi'an, Xi'an Jiaotong University Press)